

## Upper Crustal Structure in the Torni-Purnad Region, Central India Using Magnetotelluric Studies

C. K. RAO, S. G. GOKARN, and B. P. SINGH

*Indian Institute of Geomagnetism, Colaba, Bombay 400 005, India*

(Received May 27, 1993; Revised January 12, 1995; Accepted January 28, 1995)

Magnetotelluric studies were conducted over a 100 km long NS profile in the Satpura range and Tapti basin. Data were collected at 18 stations in this region with an interstation spacing of 3–10 km. The geoelectric substructure was obtained using a two dimensional modelling technique and has indicated the presence of Deccan traps and Gondwana sediments overlying a rather complex granitic basement. Two distinct layers of Deccan basalts were delineated with a total thickness varying from 2000 m in the central part to about 300–1000 m on either sides of this NS trending profile. The thickness of the Gondwana sediments below the traps was observed to vary rather strongly in the range, 300–2000 m. Two vertical conductive zones were delineated corresponding to the Khandwa lineament and the Burhanpur tear but the sensitivity studies indicated a large degree of nonuniqueness associated regarding the shape and vertical extent of these conductors. An interesting finding of these studies is the presence of a prism shaped body in the central part of the survey profile in the Satpura horst region at depths between 3.5 and 14 km with a resistivity of 20 ohm-m. The body had a lateral extent of 8 km at the top and 40 km at the bottom in the NS direction. This observation is discussed along with the other geophysical results in the Satpura and Tapti regions.

### 1. Introduction

The Narmada-Son-Tapti lineament zone is one of the most prominent features on the tectonic and geological map of India. This ENE-WSW trending mega lineament is a line of weakness with the regions on the north and south moving vertically as well as laterally (Ravishanker, 1987). The Satpura range forms the prominent Satpura horst block flanked by actively subsiding grabens: the Tapti-Purna graben on the south and the Narmada graben on the north and extends in almost an EW direction between the longitudes 75°E and 78°E. The Bouguer, free air and isostatic anomaly maps indicate a positive anomaly as against an expected negative anomaly on this mountain range, indicating an anomalous crust below the Satpura horst structure. Verma (1985) carried out gravity modelling studies and observed that this could be explained under the assumption of a higher upper crustal density of +0.06 over the normal value. He has justified the assumed higher crustal density on the basis of historically different evolution of the crust in the Satpura range from that in the surrounding region.

Major parts of the Tapti graben and the Satpura range is covered by the Deccan basalts of varying thickness overlying the Gondwana sediments. In some parts however a thin layer of recent alluvial deposits may be encountered overlying the Deccan basalts as shown in Fig. 1. Intense faulting is observed in this region due to the long history of tectonic activity, most of the faults being along the ENE-WSW direction (Ravishanker, 1987).

The deep seismic sounding studies (Kaila *et al.*, 1985) across the Satpura and Tapti region along the profile shown in Fig. 1 have delineated 400–1000 m thick Deccan traps covering about 1.7 km thick Gondwana sediments. The direct current (DC) resistivity studies have reported about 300–1600 m thick basaltic cover over the Gondwana sediments (Nayak *et al.*, 1985). However in the central part of the Satpura horst, they have reported less than about 300 m of Gondwana sediments.

With an intention of probing the deeper electrical resistivity structure magnetotelluric studies were

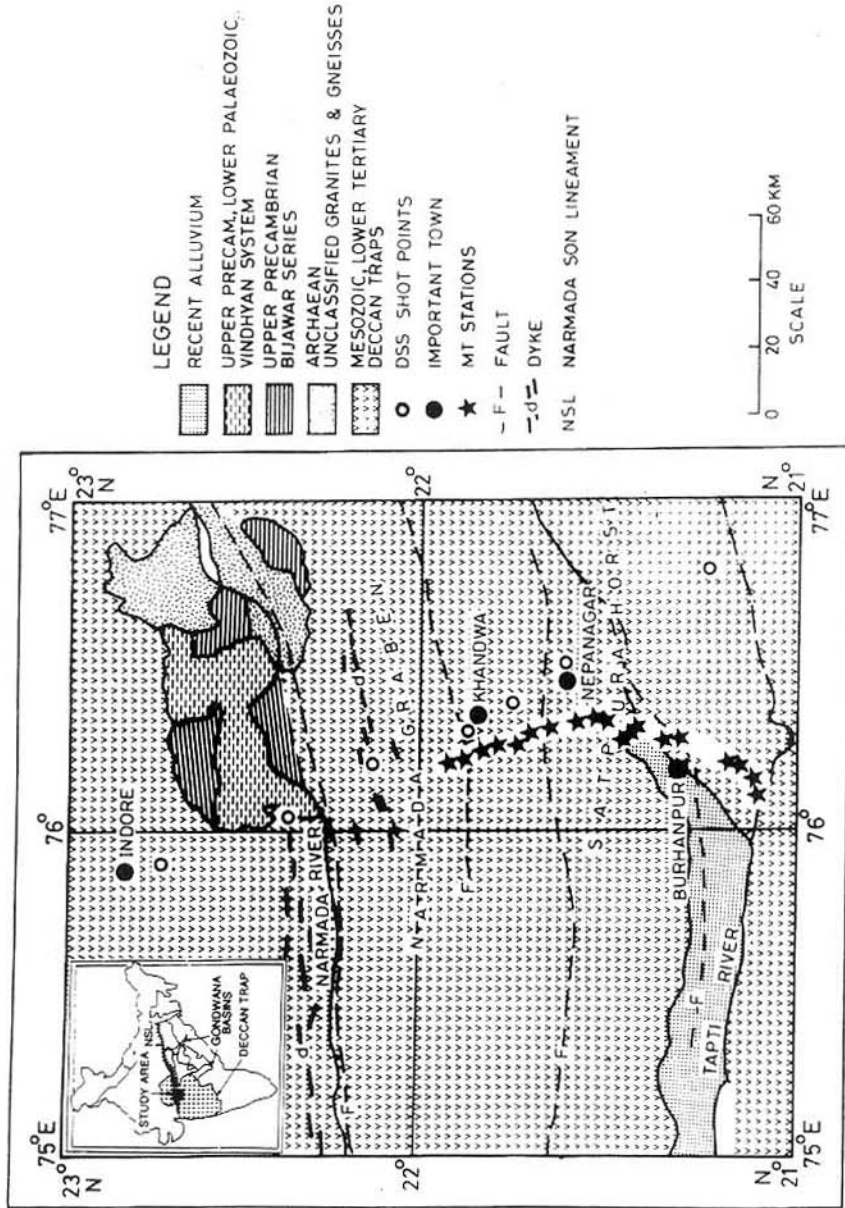


Fig. 1. Geological and tectonic map showing the magnetotelluric survey profile.

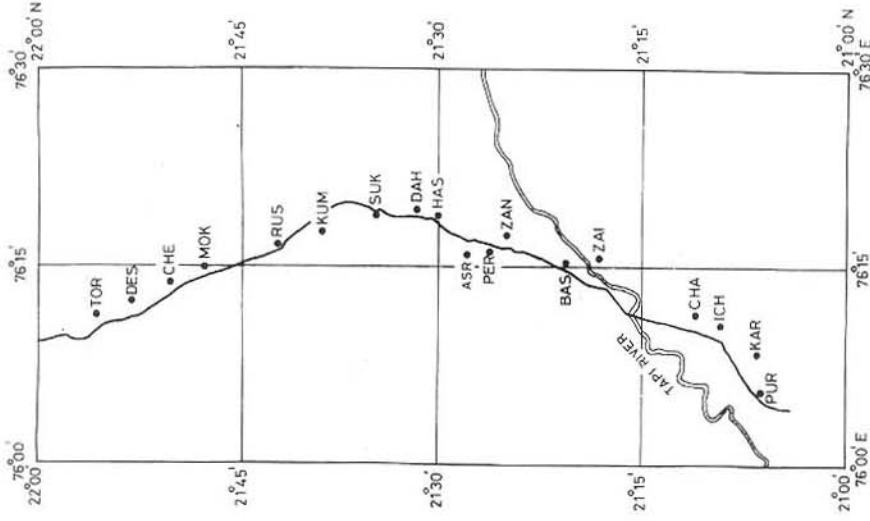


Fig. 2. Location map of the MT stations over the Tornj-Purnad profile.

undertaken along a 100 km long linear profile between Torni and Purnad. Data were collected at 18 stations along this line with an interstation spacing of 3–10 km (Fig. 2). The entire survey profile is in the Deccan trap region.

## 2. Experimental and Analysis Techniques

The magnetotelluric studies were conducted using the short period automatic magnetotelluric (SPAM) system supplied by the University of Edinburgh (U.K.) in the frequency range, 128–0.01 Hz. This range was grouped into four frequency bands; with band-widths of 128–16 Hz, 16–2 Hz, 2–0.25 Hz and 0.25–0.01 Hz and the corresponding sampling intervals of 512, 64, 8 and 1 samples per second respectively. At least 50 windows of 256 samples were used for obtaining the response functions (apparent resistivity, phase, skew etc.). The conventional analysis procedure described by Vozoff (1972) was used here. The electric field components were measured using the copper-copper sulphate probes where as the induction coil magnetometers were used for measuring the magnetic field components.

## 3. Regional Strike Estimates

The skew of impedance ( $S = |Z_{xx} + Z_{yy}|/|Z_{xy} - Z_{yx}|$ ) averaged throughout the frequency range of investigation was smaller than 0.01 at all stations and the largest value of skew at any of the frequencies was 0.25 at all stations. Further the apparent resistivities in the two orthogonal directions were in general different. In view of this fact the geoelectric substructure was assumed to be two-dimensional.

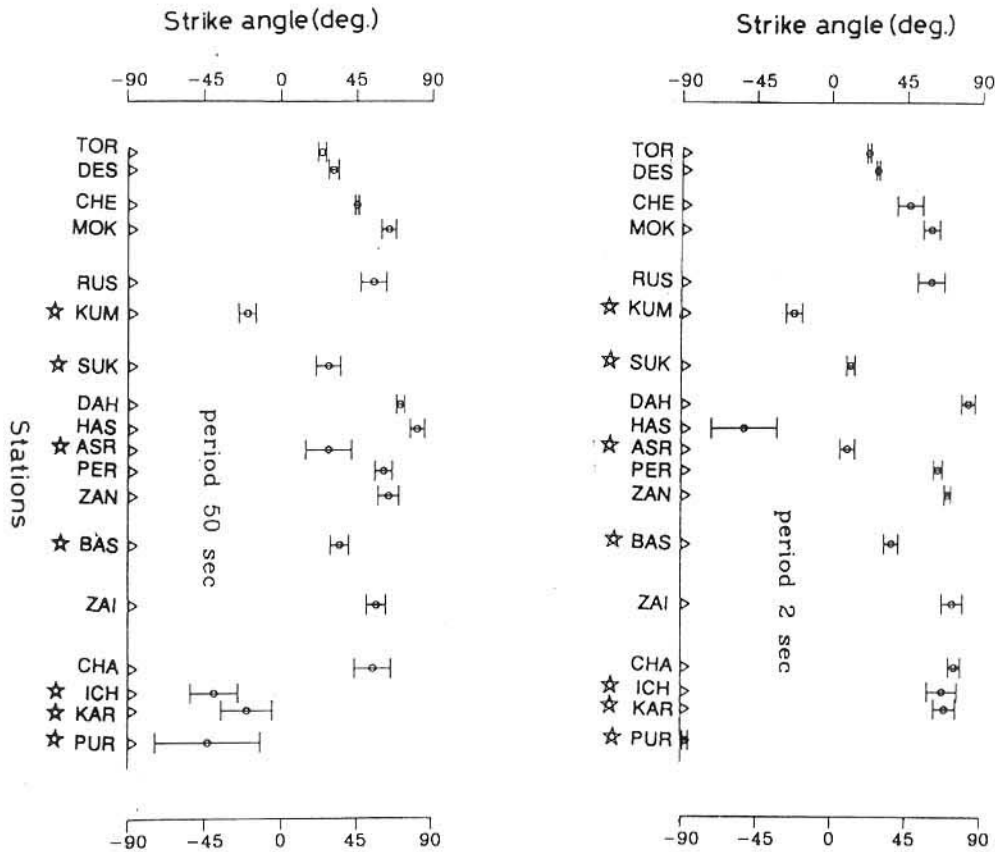


Fig. 3. The average strike angle at all the stations on the survey profile (in degrees from north) which is also the direction of the minor resistivities. The stations marked by stars had the major:minor resistivity ratios of 1.5–3 and thus were assumed to show a one dimensional resistivity structure.

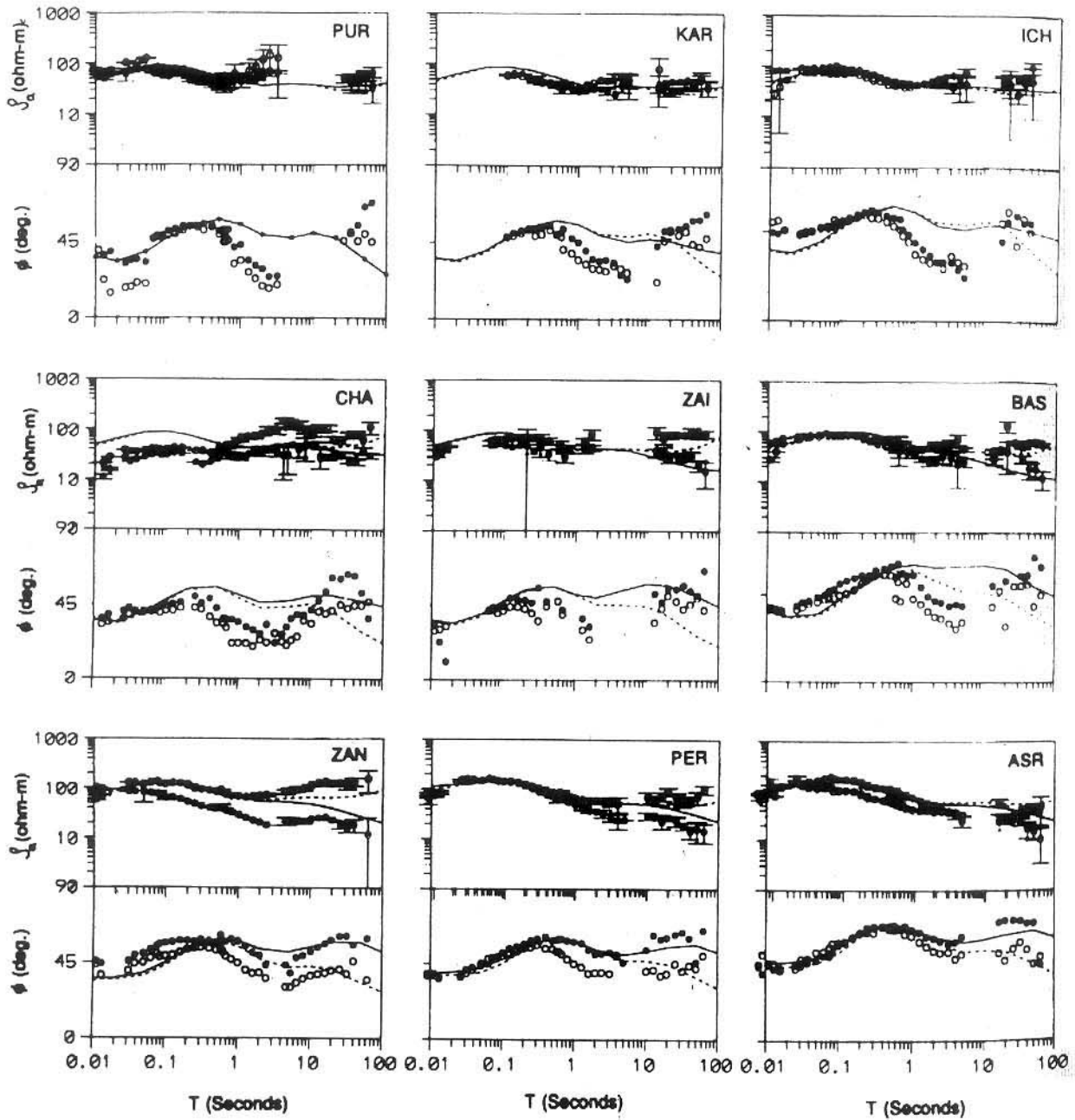


Fig. 4a. Apparent resistivity and phase variations with period in the  $E$ - (solid circles) and  $H$ -polarisations (open circles). The solid and dashed lines are the fits to the apparent resistivities in the  $E$ - and  $H$ -polarisations respectively obtained using the two dimensional forward modelling.

The strike direction at each of the stations was determined by rotating the impedance tensor at all the frequencies so as to minimize the diagonal elements ( $Z_{xx}$  and  $Z_{yy}$ ). The major and minor axis were predominantly aligned along  $N30^\circ \pm 10^\circ W$  and  $N60^\circ \pm 10^\circ E$  respectively at most of the stations. The rotation angles clock-wise from north for minor directions at periods 2 and 50 sec. are shown in Fig. 3. The rotation angles at short periods ( $<10$  sec.) at all the stations as also those at MOK, KAR, ICH and PUR at all periods were erratic. However in these cases the ratio of the major and minor resistivities were less than a factor of 3 indicating that geoelectric structure in these cases could be assumed to be one dimensional. In view of this and also the fact that most of the lineaments in this region are aligned along ENE-WSW (Ravishanker, 1987), the regional strike direction was assumed to be along  $N60^\circ E$  and the apparent resistivities and phases along this direction were assumed to be the  $E$ -polarisation values. The

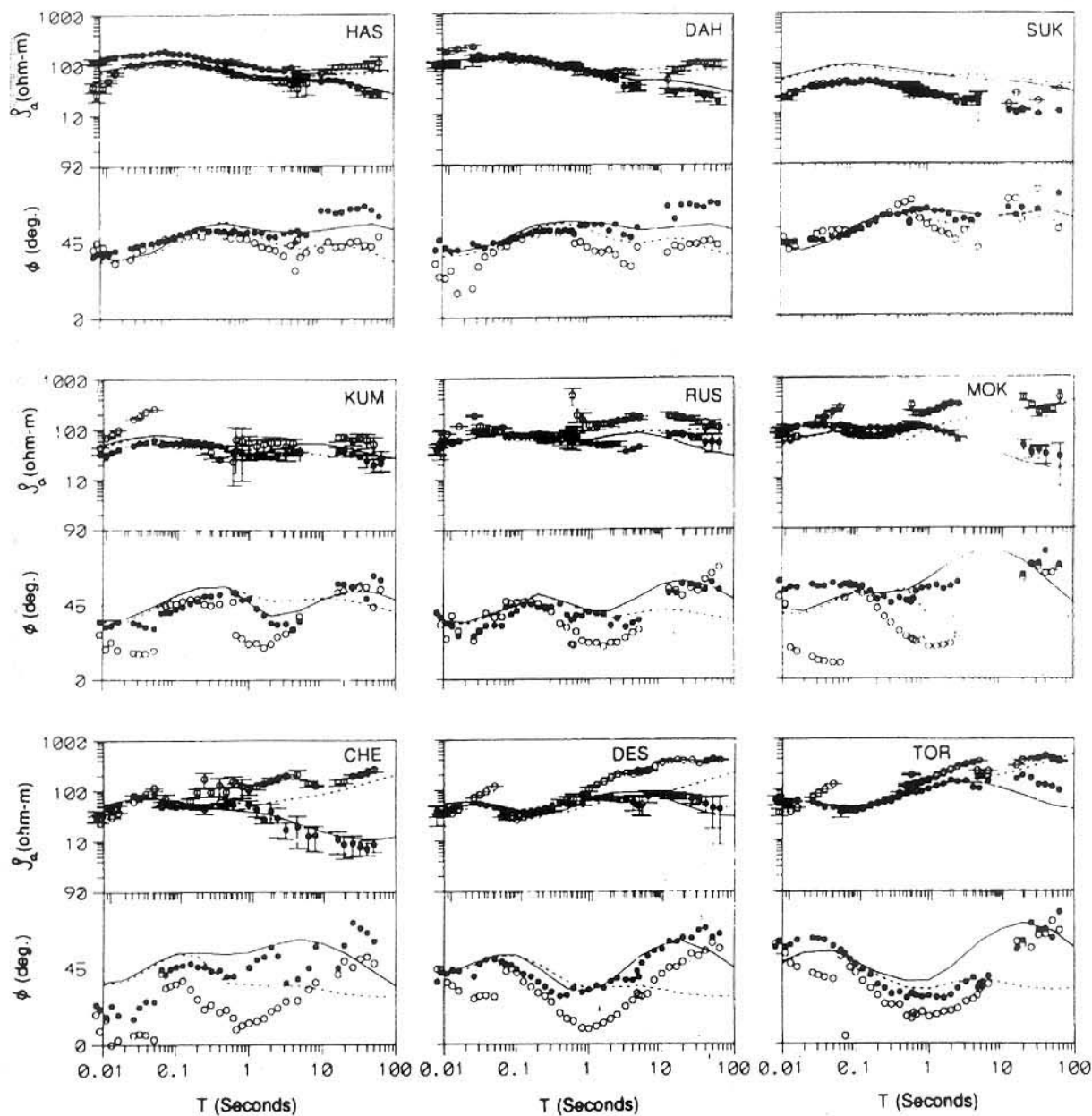


Fig. 4b. Same as for Fig. 4a.

frequency variation of rotated apparent resistivities and phases are shown in Figs. 4a and b. At some stations (TOR, DES, MOK, KUM and RUS) the apparent resistivities at high frequencies in the  $H$ -polarisation show a discontinuity at 16 Hz. This was due to some instrumentation problem which arose because of improper functioning of one of the 50 Hz power line notch filters. However the data at lower frequencies are not likely to be affected by this problem because these notch filters are switched off while recording the data at these frequencies (<16 Hz).

#### 4. One Dimensional Inversion and Static Shift Correction

The depth variation of the electrical resistivity was determined using a one dimensional modified Marquardt inversion technique (Marquardt, 1963) using the apparent resistivities and phases in the  $E$ -polarisation. These values are less influenced by the deeper lateral resistivity inhomogeneities than the  $H$ -

polarisation values. The depth-resistivity profiles at all the stations were plotted together and interpolated to obtain a preliminary geoelectric cross section (Fig. 5). Some static shift is evident at stations PER, ZAI, KAR, CHA and SUK as seen from the predominant downward bias of most of the resistivity and thickness values at these stations. The preliminary geoelectric structure shows a top conducting layer of 20–80 ohm-m overlying a resistive (150–300 ohm-m) layer. The depth to the bottom of the second layer is about 2000 m in the central part (below HAS and ASR) and decreases to 300 m on the north and 800–1000 m on the southern part of the profile. The direct current resistivity studies (Nayak *et al.*, 1985) have reported 1600 m thick Deccan basalts in the central part decreasing on the north and south to 300 and 900 m respectively. Thus it was decided to correct for the static shift by smoothening the base of the second (resistive) layer in the observed geoelectric structure by using bottom of the Deccan traps as the “Key layer parameter” as suggested by Jones (1988). It may also be noted here that the bottom of the resistive layers is a well resolved parameter in the MT response functions. The depth to the bottom of the Deccan traps between the stations on either side of the static shift affected station was linearly interpolated and the corrected depth at the affected station was estimated. Now the problem of correcting for the static shift reduces to determining the constant for the station by which all the apparent resistivities at the station are to be multiplied. To find out this constant a method based on the graphical estimation of the depth-resistivity profiles described by Kaufman and Keller (1981, pp. 541–542) was adopted. It is clear from the discussion there that the descending branch of the resistivity-period curve is strongly influenced by the depth to the bottom of the resistive layer. The “T-line” (Fig. 17.2 in Kaufman and Keller, 1981, p. 542) which is the asymptote on the descending branch corresponding to the second layer (resistive) of the apparent resistivity-period plots (*E*-polarisation) was drawn through the point of inflexion along with the T-line corresponding to the corrected depth determined as explained above. The apparent resistivities at the frequency corresponding to the point of inflexion were determined for both the T-lines. The correction factor is then the ratio of the corrected apparent resistivity to the observed value at the point of inflexion. The observed apparent resistivity curve can be shifted to the correct position by multiplying all the apparent resistivities at the station by the correction factor. The *E*-polarisation data at the stations SUK, PER, ZAI, KAR and CHA were corrected and the ratio of the corrected to observed apparent resistivities were 2.0, 1.27, 1.67, 1.33 and 2.83 respectively. The static shift corrected resistivity curves were then used to obtain the one dimensional depth-resistivity profiles and a preliminary geoelectric structure (not shown).

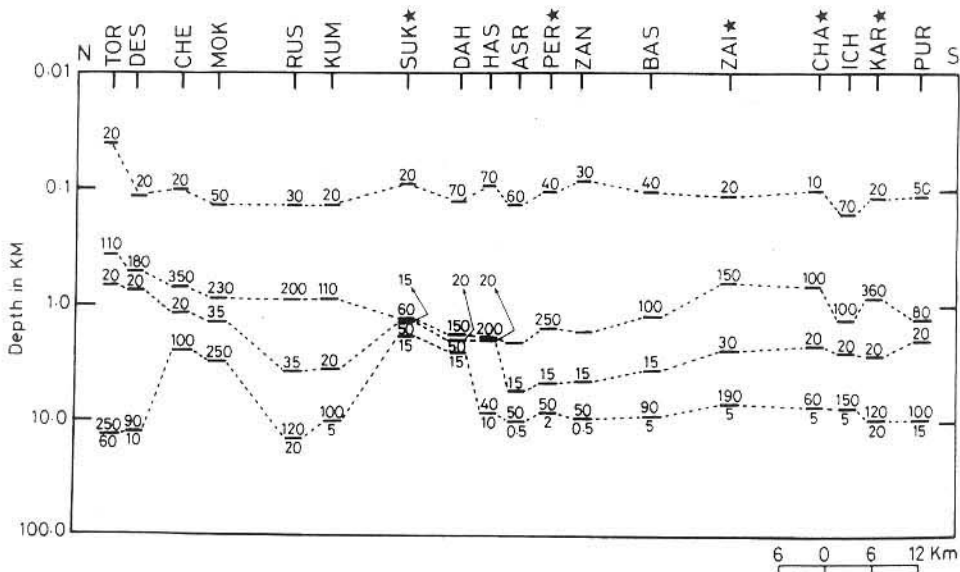


Fig. 5. Preliminary geoelectric structure obtained from one dimensional inversion of the *E*-polarisation data. The stations marked by stars (\*) were chosen for the static shift correction.

## 5. Two Dimensional Modelling

A finite difference two dimensional forward modelling program working on the principles similar to those described for a three dimensional modelling scheme by Madden and Machie (1989) was used for obtaining the final geoelectric cross section (Fig. 6) using the static shift corrected data. Here a two dimensional model was formulated on the basis of the preliminary geoelectric structure obtained earlier and the model parameters were changed so as to obtain a good fit between the observed and computed spatial and period variations of apparent resistivities in both the  $E$ - and  $H$ -polarisations at all the stations and at periods 1, 10 and 100 sec. The spatial variation of the apparent resistivities along with the fits obtained for the final two-dimensional model are shown at periods, 1, 10 and 100 sec. in Fig. 7. The modelled apparent resistivities in  $E$ - (solid lines) and  $H$ -polarisations (dashed lines) are shown in Figs. 4a and b for the stations not corrected for static shift. Figure 8 shows the observed and static shift corrected apparent resistivities along with the modelled apparent resistivities in  $E$ -polarisation for the stations where the static shift corrections were applied.

The geoelectric substructure (Fig. 6) along the survey profile indicates a 150–200 m thick top conductive layer (40 ohm-m) overlying a more resistive (150 ohm-m) second layer. The thickness of the second layer is about 2000 m between SUK and BAS in the central part of the profile and decreases to about 300 m on the north and about 1000 m on the south. Both these layers seem to be due to the Deccan basalts with the top layer showing some sporadic weathering. The studies of the basaltic outcrops in the Mandaleshwar–Pipaljopa region about 50 km west of the present survey area identified 28 distinct basaltic flows of which the top 12 flows with a total thickness of about 100 m show sporadic weathering which

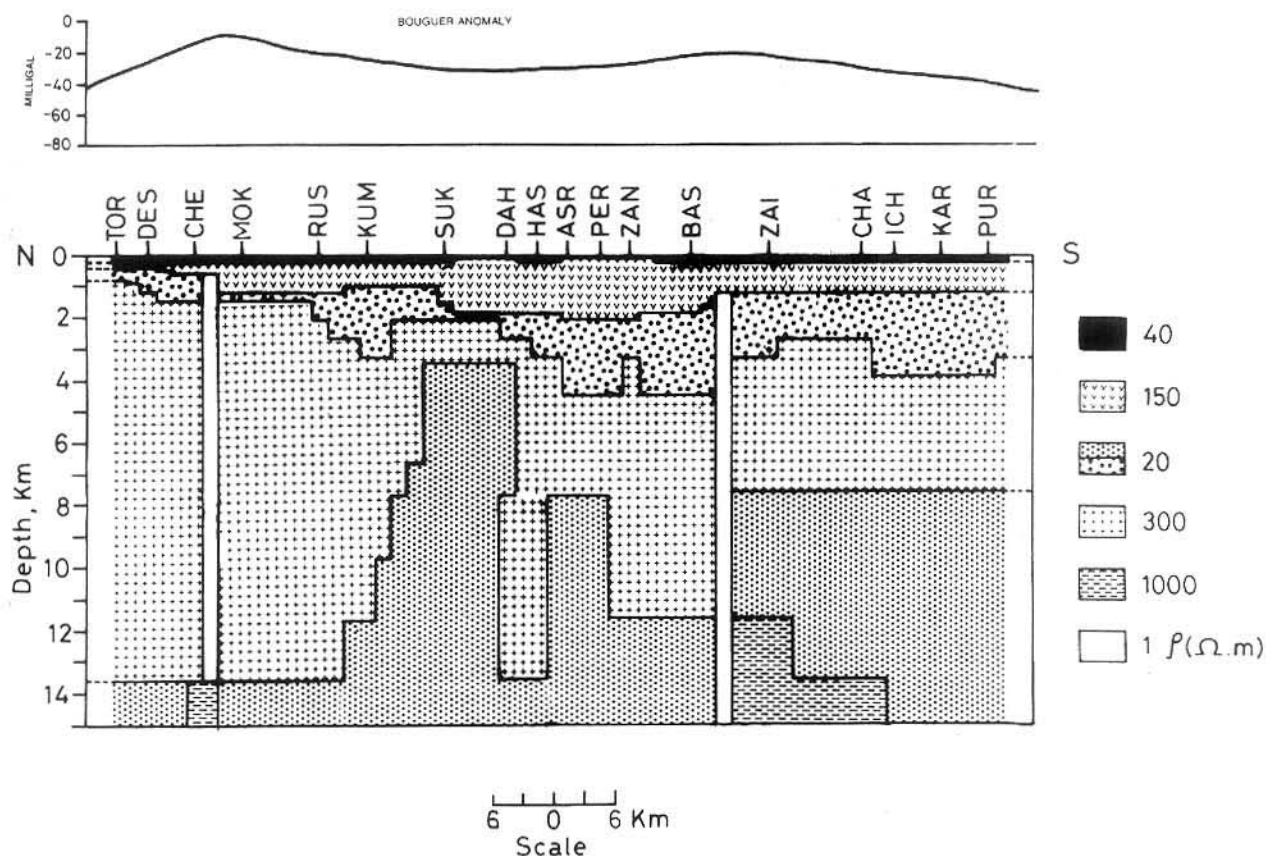


Fig. 6. Geoelectric substructure obtained by using two dimensional modelling of the static shift corrected data. The Bouguer gravity variations over the survey profile are shown in the upper part of the figure.

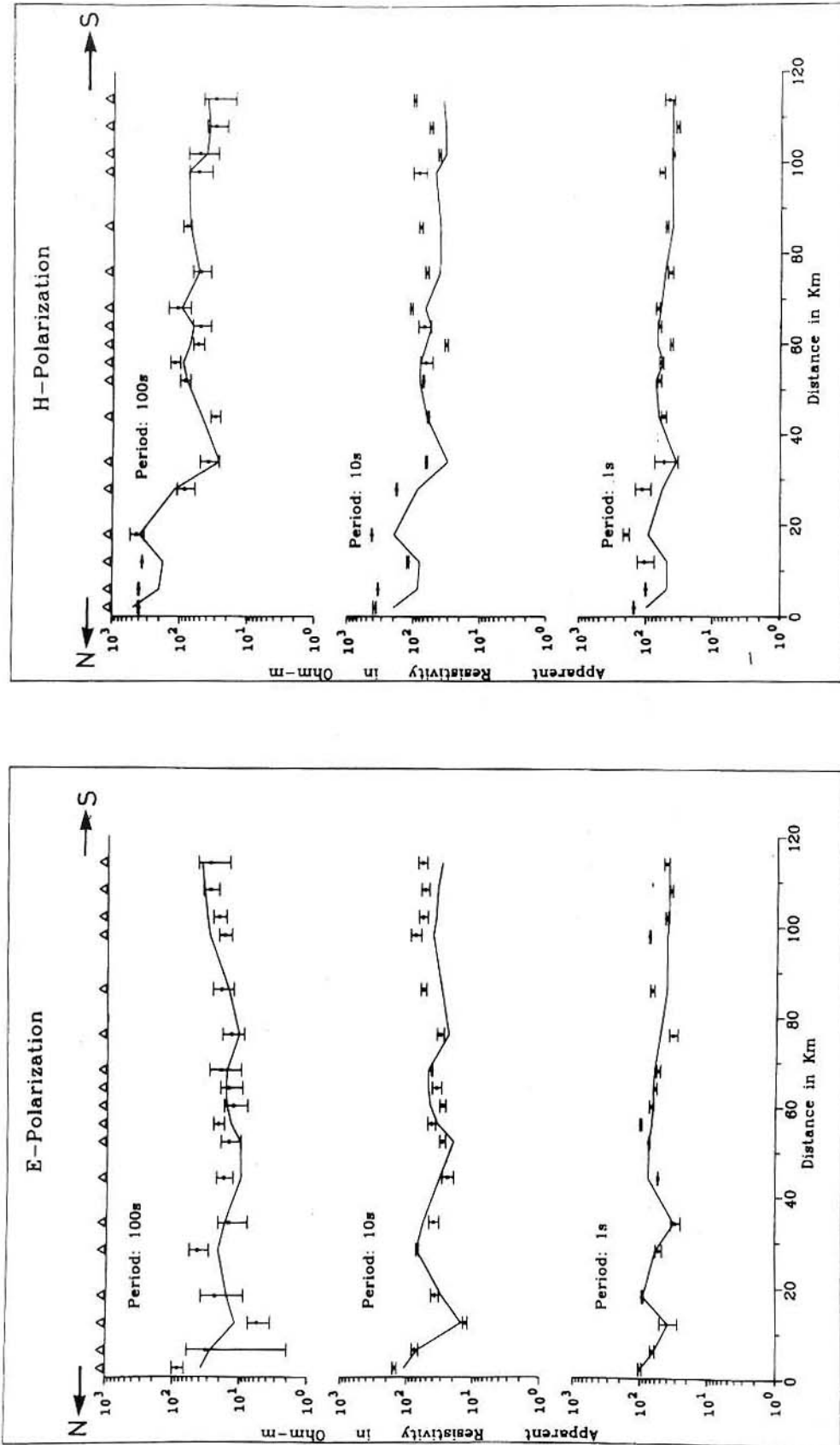


Fig. 7. Spatial variation of the apparent resistivities at 1, 10 and 100 sec. periods over the survey profile in E- and H-polarisations. The solid curve through the apparent resistivity values are the computed values for the final two dimensional resistivity structure shown in Fig. 6.



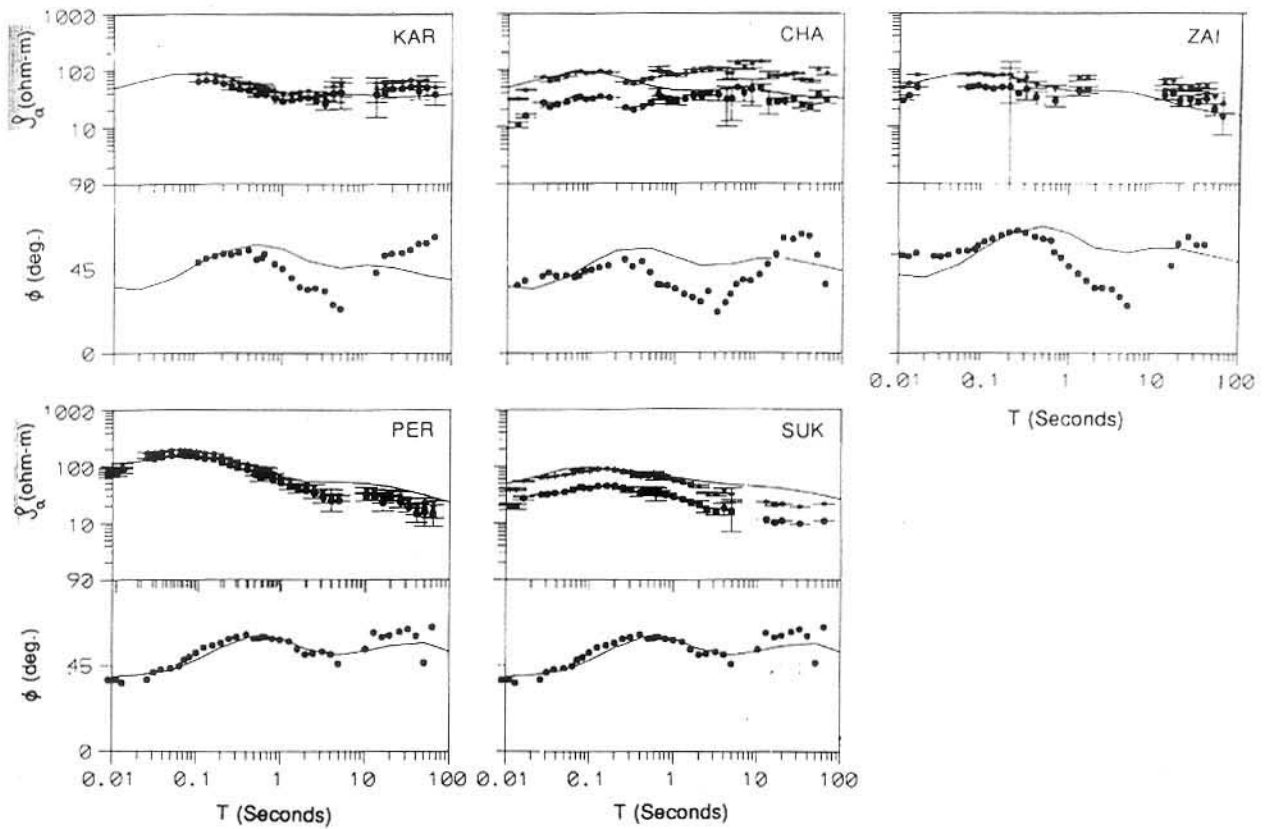


Fig. 8. Observed (circles) and static shift corrected apparent resistivities (crosses) in  $E$ -polarisation. The solid curve indicates the fit obtained from the two dimensional forward modelling.

is absent in the lower flows (Sreeniwasa Rao *et al.*, 1985). Pal and Bheemasankaram (1976) have reported the presence of 27 flows in the region north of ASR (Fig. 2). However there are no reports on the chemical composition or the physical state of these layers. In view of these studies it seems reasonable to attribute the top two layers to the Deccan traps.

Below the Deccan basalts a conducting layer (20 ohm-m) was delineated with thickness varying in the range, 200–2000 m which could be due to the Gondwana sediments. The strong variations in their thickness reflects on the long history of tectonic activity in this region (Ravishanker, 1987). This fact is also supported by the complex pretrappean topography which is evident from the strong undulations of the top of the granitic upper crust underlying the Gondwana sediments. The granitic basement had a resistivity of 300 ohm-m and thickness in the range, 10–12 km.

Two vertical resistivity contrasts were delineated, one below the stations, CHE and MOK and the second below BAS and ZAI located in the close vicinity of the Khandwa lineament and the Burhanpur tear. The sensitivity studies indicated a large degree of nonuniqueness regarding the shape, extent as well as the resistivity of these conductors. However the spatial variation of the resistivities (Fig. 7) do indicate the presence of conductive bodies at these locations. Thus it was not possible to determine the electrical character of the Khandwa lineament and the Burhanpur tear from the present studies.

A prism shaped conductive feature having a resistivity of 20 ohm-m was delineated below the stations RUS and BAS. The top of this conductive body was about 8 km wide extending from DAH to ASR and located at depth of 3.5 km from the surface. At its base 14 km below the surface, this conductive structure had a lateral extent of 40 km in the NS direction. The structure seemed to be composed of two distinct conductive zones rising from the lower crustal depths to the surface, one from between the stations RUS and DAH and the other between BAS and ASR and converging towards each other at shallow depths. The heat flow data in this region indicates that the entire survey region has a heat flow in the range, 100–180

mW/m<sup>2</sup> (Ravishanker, 1988). However there are no reports regarding the variation of the heat flow over the present profile. The conductive feature observed here is located on the gravity low (Fig. 6) on the northern part of the Satpura range and may be due to entrapment of fluids in the fractured zones of the granitic upper crust in the course of the long tectonic history of this region. However the detailed heat flow measurements may be useful in understanding this feature.

## 6. Conclusions

The magnetotelluric studies across the Satpura range and Tapti basin have been presented here. The Deccan traps are observed to be about 2000 m thick in the central part of the survey profile with their thickness decreasing to 300 m on the north and 1000 on the south of the profile. The Gondwana sediments below the Deccan basalts were observed to have thickness varying from 300–2000 m. The strong variations of the thickness of the Deccan traps and Gondwana sediments are indicative of the long history of tectonic activity experienced by this region. A conductive feature was delineated at depths between 3.5 and 14 km located in the granitic crust coinciding with a local gravity low of 25–30 mGal. The survey region falls in a high heat flow zone with heat flows of about 100–180 mW/m<sup>2</sup>. In view of these facts the observed conductive feature was attributed to some lower crustal fluids which might have been released in to the fractures in the granitic upper crust.

The authors express a deep sense of gratitude to Prof. T. R. Madden and Dr. R. L. Machie for providing the two-dimensional modelling program. Some excellent suggestions made by the referees of this paper are gratefully acknowledged. Thanks are also due to M/s C. Selvaraj and R. N. Javeri for their help in field work and Mr. K. Vijay Kumar and Dr. P. B. V. Subba Rao for some useful discussions.

## REFERENCES

- Jones, A. G., Static shift of magnetotelluric data and its removal in a sedimentary basin environment, *Geophysics*, **53**, 967–978, 1988.
- Kaila, K. L., P. R. Reddy, M. M. Dixit, and P. Koteswara Rao, Crustal structure across the Narmada-Son lineament, Central India, *J. Geol. Soc. India*, **26**, 465–480, 1985.
- Kaufman, A. A. and G. V. Keller, *The Magnetotelluric Sounding Method*, Elsevier Amsterdam, 1981.
- Madden, T. R. and R. L. Machie, Three dimensional magnetotelluric modelling and inversion, *Proc. IEEE*, **77**, 318–333, 1989.
- Marquardt, D. W., An algorithm for least square estimation of the nonlinear parameters, *J. Soc. Indust. Appl. Math.*, **11**, 431–441, 1963.
- Nayak, P. N., K. K. Dutta, Ravishanker, and M. N. Sehgal, Geological and geophysical studies vis-a-vis results of the DSS profiles in central India, an analysis, in *Proc. Int. Symp. on Deep Seismic Sounding Traverses*, edited by K. L. Kaila and H. C. Tiwari, pp. 83–97, Assoc. Expl. Geophys., Hyderabad, India, 1985.
- Pal, P. C. and V. L. S. Bheemasankaram, Tectonics of the Narmada-Son-Brahmaputra lineament, *Geol. Surv. India Misc. Publ.*, No. 34, 133–140, 1976.
- Ravishanker, Neotectonic activity along the Tapti-Satpura lineament in central India, *Indian Minerals*, **41**, 19–30, 1987.
- Ravishanker, Heat flow map of India and discussions on its geological and economic significance, *Indian Minerals*, **42**, 89–110, 1988.
- Sreeniwas Rao, M., N. Rama Subba Reddy, K. V. Subba Rao, C. V. R. K. Prasad, and C. Radhakrishna Murthy, Chemical and magnetic stratigraphy of parts of Narmada region, Deccan basalt province, *J. Geol. Soc. India*, **26**, 617–639, 1985.
- Verma, R. K., Gravity field, DSS and crust-mantle relationship in peninsular India, in *Proc. Int. Symp. on Deep Seismic Sounding Traverses*, edited by K. L. Kaila and H. C. Tiwari, pp. 27–41, Assoc. Expl. Geophys., Hyderabad, India, 1985.
- Vozoff, K., Magnetotelluric studies in the sedimentary basins, *Geophysics*, **37**, 98–141, 1972.